Technical Paper

ISSN 1997-1400 Int. J. Pavement Res. Technol. 8(5):353-362

Local Calibration of a Permanent Deformation Model for Asphalt Pavements Using Long-term Field Data

Qiang Li [1+], Xiang Ma [1], and Guofen Li [1]

Abstract: A permanent deformation model of asphalt pavements based on shear properties was locally calibrated and validated using long-term field data in Jiangsu of China. The detailed information on the climate, traffic, distresses, pavement structures, and materials for 24 pavement sections from 4 main lines in highway network was widely investigated. The required material parameters in the prediction model including dynamic modulus $|E^*|$, cohesion, and friction angle were directly measured on 9 types of asphalt mixtures in laboratory. The hourly pavement temperature field in each analysis period was predicted using a transient finite element method model based on heat transfer theory. The sub-season concept based on normal frequency distribution function was employed to consider the effects of extreme temperatures. A conversion equation of axle load based on rutting equivalent principle was developed for traffic characterization. Traffic wander and load frequency distribution were also carefully considered in the calibration process. After statistical optimization using a three-step procedure the optimum combination of calibration factors were obtained by minimizing the sum of squared errors between the predicted and measured permanent deformation. It is found from the validation research that the locally calibrated model can provide reasonable predictions for various asphalt pavements and satisfy the accuracy requirement in engineering practice.

DOI: 10.6135/ijprt.org.tw/2015.8(5).353
Key words: *Asphalt pavement; Calibration factors; Permanent deformation; Shear properties.*

Introduction

Permanent deformation or rutting due to repeated traffic loading is one of the major distresses in asphalt pavements. It not only results in a loss of pavement service lives but also reduces safety and convenience of traffic [1-2]. Asphalt concrete layers usually contribute a major part to the total rutting among various pavement structure layers, especially in China where the semi-rigid base and subbase are widely used.

Many attempts have been made to predict the permanent deformation of asphalt concrete using the laboratory testing results [3-6]. The permanent deformation models can be roughly divided into three categories. The first category is empirical models, represent by the power law model [3] and Zhou's three-stage model [4]. These models correlate the cumulative permanent strain with the number of load cycles using statistical methods. Although they are easy to use, the regression coefficients greatly depend on material properties, temperatures, and loading conditions. The second category is mechanical-empirical models, which are increasingly concerned. The most famous example is the Mechanistic-empirical pavement design guide (MEPDG) model [5]. It incorporates the mechanical term (resilient strain) to reflect the effect of pavement responses except the empirical regression. However, the resilient strain is not the main mechanical response to cause the permanent deformation and it cannot accurately characterize the effect of pavement structures and material properties. The third category is theoretical models, which are mainly based on viscoelastic mechanics and finite element method (FEM). They can successful describe the permanent deformation behavior, however, the complexity in determining the material parameters limits their application [6].

Shear flow is a dominant contributor to permanent deformation in asphalt concrete layers [7]. Therefore, shear properties of asphalt mixtures should be incorporated into the permanent deformation prediction for asphalt pavements. A permanent deformation model of asphalt concrete based on the ratio of shear stress to strength was established in authors' previous work [8-9]. The triaxial compressive strength (TCS) and repeated-load permanent deformation (RLPD) tests on three types of asphalt mixtures with varying volumetric properties were performed in laboratory to correlate shear properties with rutting performance. This model can successfully predict the permanent deformation of various asphalt mixtures all the way up to failure under a wide range of loading and temperature conditions without changing model coefficients. Then, it was preliminarily calibrated by an accelerated pavement testing (APT) conducted on a typical pavement structure at various temperatures.

APT can simulate field conditions to a certain extent, however, there are some differences existing between them, such as loading time, rest duration, traffic distribution (wandering), the change of environment conditions over time, and age hardening of asphalt [10]. Therefore, APT is not capable of completely capturing actual long-term pavement performance and deterioration mechanism. The performance prediction model should be recalibrated for local pavement structure, material, traffic, distress, and environmental conditions [11].

The main objective of this study is to calibrate the permanent deformation model for asphalt pavements based on shear properties

[1] School of Civil Engineering, Nanjing Forestry University, Longpan Road 159#, Nanjing, China, 210037.
[+] Corresponding Author: E-mail lq2526@163.com
Note: Submitted October 15, 2014; Revised August 2, 2015; Accepted August 4, 2015.

using long-term field data in Jiangsu of China. To accomplish this objective, the long-term pavement performance of the main lines in Jiangsu highway network was widely investigated. Three types of laboratory tests were conducted in laboratory to measure the required material parameters in the prediction model. Some important factors such as conversion of axle load, pavement temperature field, traffic wander, and statistical optimization method were carefully considered in the calibration process. Finally, the model with the optimum calibration factors was validated using another independent data set.

Proposed Permanent Deformation Model Based on Shear Properties

Based on the Mohr-Coulomb failure theory, the ratio of shear stress to strength for asphalt mixtures is defined as how far the actual stress at potential failure plane is from the failure envelope for a specific confining pressure, as shown in Fig. 1. It can be calculated as follows [8]:

$$\tau/\tau_f = \frac{(\sigma_1 - \sigma_3)(\tan\varphi\sin\varphi + \cos\varphi - \tan\varphi)}{2(c + \sigma_3\tan\varphi)} \tag{1}$$

where τ/τ_f is the ratio of shear stress to strength; σ_1 is actual maximum principal stress, kPa; σ_3 is actual minimum principal stress, kPa; c is cohesion, kPa; φ is friction angle, °.

From laboratory tests results, a nice exponential correlation between the ratio of shear stress to strength and permanent strain of asphalt mixtures under a given load cycle was observed. A permanent deformation model based on the ratio of shear stress to strength was then developed and calibrated using APT data [9]. It was finally expressed as:

$$\varepsilon_p = 0.0092675 e^{0.0000062807N} e^{3.6723\tau/\tau_f N^{0.1032}} t^{0.4224} \tag{2}$$

where ε_p is permanent strain; N is the number of load cycles; t is load duration of each cycle, s; e is natural exponential base (≈ 2.718).

It is found from Eq. (2) that the permanent deformation of asphalt pavements is only a function of the ratio of shear stress to strength, number of load cycles, and load duration of each cycle in the proposed prediction model.

Field Data Collection

After the explosive development over the past twenty years, the Jiangsu highway network has been formed and the total mileage exceeds 4,000 km. The Pavement Management System (PMS) has been developed for the main lines in Jiangsu highway network, in which very detailed information about pavement structures, materials, traffic, climate, long-term performance, maintenance, and rehabilitation have been collected. It supplies the authors an adequate source to make the potential calibration.

It is well known that the quality of the data plays a major role in the calibration accuracy [12]. Therefore, there are some basic principles accepted in this study to select proper pavement sections for calibration analysis. Pavement sections must exhibit distinct rutting in a reasonable amount of time. Only rut data observed in the right truck lanes are used. The consecutive and complete information must be collected. No significant rehabilitations or maintenance activities have taken place from opening to traffic until the investigation time.

Finally, a total of 24 pavement sections from 4 highways with time series rut data 181 points were selected in the analysis after a careful data examination on the PMS database. The map in Fig. 2 shows that it covers all three representative geographic regions (north, middle, and south) of Jiangsu. A split-sample approach was

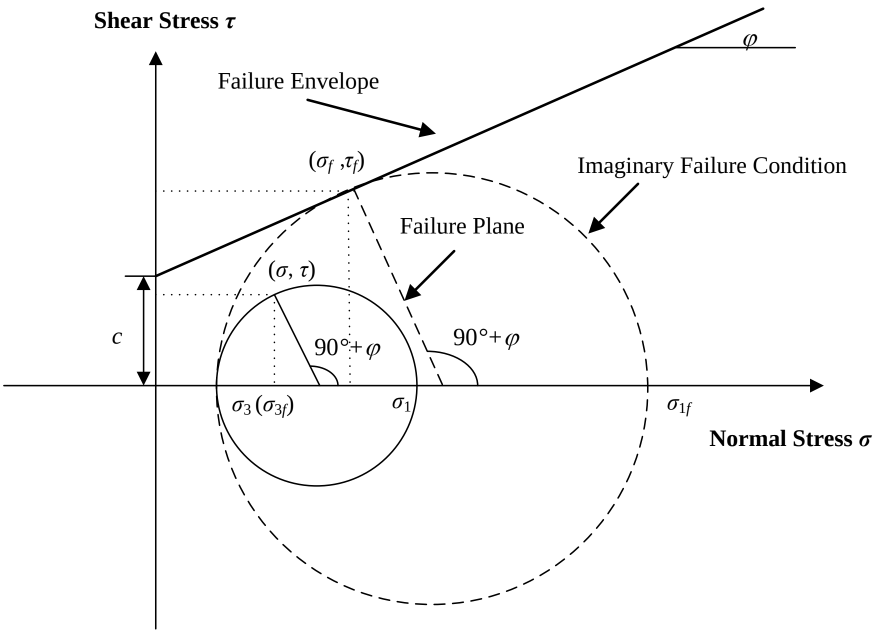

Fig. 1. Definition of the Ratio of Shear Stress to Strength [8].

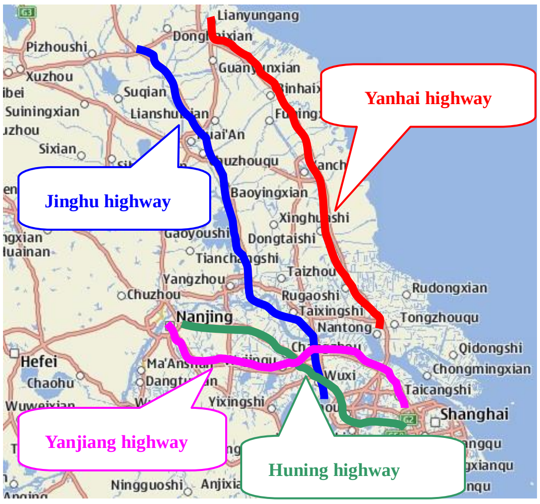

Fig. 2. Location of Selected Pavement Sections.

used during calibration process [13]. The 20 pavement sections from the Jinghu (JH), Huning (HN), and Yanhai (YH) highways were used for calibration purpose and the rest 4 pavement sections from the Yanjiang (YJ) highway were kept aside for validation purpose. The pavement structures of these sections are provided in Table 1.

All pavement sections consisted of four main structure layers: asphalt concrete surface (top, middle, and bottom), base, subbase and subgrade. Typically, semi-rigid materials such as cement stabilized macadam (CSM) or lime-fly ash stabilized macadam (LFSM) was used in base while lime-fly ash soil was used in subbase. For some trial sections, asphalt treated base (ATB) was also selected in top base. Different types of aggregate gradations were designed for asphalt mixtures in three asphalt concrete sublayers, such as stone mastic asphalt (SMA), Superpave (Sup), non-skid asphalt course (AK), and dense graded asphalt course (AC) mixtures. Asphalt binder used were conventional PG 64-22 (C) and styrene–butadiene–styrene modified PG 76-22 (M). The asphalt mixtures shown in Table 1 were named as gradation type + nominal maximum aggregate size + binder type.

Climate data were obtained from weather stations located near each section. Traffic data were collected from the Jiangsu highway toll system. Traffic volume was determined using path split and recognition technique based on negotiation method [14]. Annual average daily traffic (AADT), vehicle classification percentages, monthly adjustment factors, direction distribution factor, and lane distribution factor were calculated. Axle load spectra for the given axle type (single, tandem, tridem, etc.) and number of axles per truck were characterized by actual axle load data collected at weigh-in-motion (WIM) stations. Rut depths were periodically measured using a 3 m-straightedge in the early years and later by a high speed APRES laser profilometer at intervals of 10 m.

Laboratory Tests

Three types of laboratory tests including the dynamic modulus |E*|, uniaxial compressive strength (UCS), and indirect tensile (IDT) strength tests were conducted to measure the required material parameters in the prediction model.

Table 1. Pavement Structures of Selected Sections.

ID	Open to Traffic	Surface			Base/Subbase
		Top	Middle	Bottom	
JH-1	2000.12	4 cm AK-16M	5 cm AC-25C	7 cm AC-25C	34 cm LFSM/40 cm LFS
JH-2	2000.12	4 cm AK-16M	5 cm AC-25C	7 cm AC-25C	36 cm LFSM/40 cm LFS
JH-3	2000.12	4 cm SMA-16M	5 cm AC-25C	7 cm AC-25C	36 cm LFSM/40 cm LFS
JH-4	2000.12	4 cm AK-16M	5 cm AC-25C	7 cm AC-25C	37 cm LFSM/40 cm LFS
JH-5	2000.12	4 cm SMA-16M	5 cm AC-25C	7 cm AC-25C	37 cm LFSM/40 cm LFS
JH-6	2000.12	4 cm AK-16M	5 cm AC-25C	7 cm AC-25C	37 cm LFSM/40 cm LFS
HN-1	2006.1	4 cm SMA-13M	6 cm Sup-20M	8 cm Sup-25C	40 cm CSM/40 cm LFS
HN-2	2006.1	4 cm SMA-13M	6 cm Sup-20M	8 cm Sup-25C	20 cm ATB + 20 cm CSM/40 cm LFS
HN-3	2006.1	4 cm SMA-13M	6 cm Sup-20M	8 cm Sup-25C	40 cm CSM/40 cm LFS
HN-4	2006.1	4 cm SMA-13M	6 cm Sup-20M	8 cm Sup-25C	36 cm CSM/40 cm LFS
YH-1	2006.10	5 cm SMA-13M	6 cm Sup-20M	10 cm Sup-25C	40 cm CSM/40 cm CSM
YH-2	2006.10	4 cm SMA-13M	6 cm AC-20M	10 cm AC-25C	38 cm CSM/40 cm LFS
YH-3	2006.10	4.5 cm AK-13M	6 cm AC-20M	10 cm AC-25C	12 cm ATB + 20 cm CSM/40 cm CSM
YH-4	2006.10	4.5 cm AK-13M	6 cm AC-20M	10 cm AC-25C	38 cm CSM/40 cm LFS
YH-5	2006.10	4 cm SMA-13M	6 cm AC-20M	8 cm AC-25M	38 cm CSM/40 cm LFS
YH-6	2005.11	4 cm SMA-13M	6 cm AC-20M	8 cm AC-25M	38 cm CSM/40 cm LFS
YH-7	2005.11	4 cm SMA-13M	6 cm SUP-20M	8 cm AC-25C	40 cm CSM/40 cm LFS
YH-8	2005.11	4 cm AK-13M	6 cm AC-20M	8 cm AC-25C	40 cm CSM/40 cm LFS
YH-9	2005.11	4 cm AK-13M	6 cm AC-20M	8 cm AC-25M	38 cm CSM/40 cm LFS
YH-10	2005.11	4 cm AK-13M	6 cm AC-20M	8 cm AC-25C	38 cm CSM/40 cm LFS
YJ-1	2004.11	4 cm AK-13M	6 cm AC-20M	8 cm AC-25M	36 cm CSM/40 cm LFS
YJ-2	2004.11	4 cm SMA-13M	6 cm AC-20M	8 cm AC-25M	40 cm CSM/40 cm LFS
YJ-3	2004.8	4 cm SMA-13M	6cm AC-20M	8 cm AC-25M	40 cm CSM/40 cm LFS
YJ-4	2004.8	4 cm AK-13M	6cm AC-20M	8 cm AC-25M	40 cm CSM/40 cm LFS

Materials

Totally, 9 types of asphalt mixtures were used in different asphalt concrete sublayers of pavement sections investigated in this study, as listed in Table 1. However, neither plant mixtures nor raw materials were available to make specimens and run the laboratory tests, because all pavement sections had finished construction before this study started. Instead, all mixtures were mixed using the same materials as field construction according to job mix formulae and compacted using a Superpave Gyratory Compactor (SGC) in laboratory. The aggregate gradations are shown in Fig. 3.

Tests and Results

Dynamic Modulus |E| Test*

A dynamic modulus |*E**| master curve is required as an input variable for a structural responses analysis. In this study, the uniaxial dynamic modulus |*E**| test was conducted with frequencies of 25, 10, 5, 1, 0.5, and 0.1 Hz at temperatures of -10℃, 5℃, 20℃, 35℃, and 50℃, respectively. With the aid of Excel Solver function, the |*E**| master curves for all mixtures as shown in Fig. 4 were constructed by a sigmoid function [15].

UCS and IDT Strength Tests

Shear strength parameters (cohesion and friction angle) are required to calculate the ratio of shear stress to strength as shown in Eq. (1). In this study, the simplified method based on the UCS and IDT strength tests was used for calculation [9]. Both tests were run at a load rate of 50 mm/min at temperatures of 40℃, 50℃, and 60℃. The cohesion and friction angle at a given temperature were predicted using the following regression equations:

$$c = \alpha_1 T^{\alpha_2} \tag{3}$$

$$\varphi = \beta_1 T^{\beta_2} \tag{4}$$

where T is temperature, ℃; α_1, α_2, β_1, and β_2 are regression coefficients provided in Table 2.

The coefficient of determination R^2 values for all cases are higher than 0.92, which indicating that Eqs. (3) and (4) supply nice predictions in a wide range of temperatures and materials.

Calibration

The calibration procedure as shown in Fig. 5 was used in this study. Several important factors in the calibration process were carefully considered and introduced in the following sections.

In this step-by-step procedure, the valid field information on climate, material, structure, and traffic was firstly investigated and processed. Then, a FEM was introduced to predict the pavement temperature field. Materials parameters were measured in laboratory followed by pavement responses calculation. Next, pavement distresses were predicted using the proposed model after conversion of axle load. Finally, the local calibration factors were obtained by comparing measured and predicted pavement distresses data.

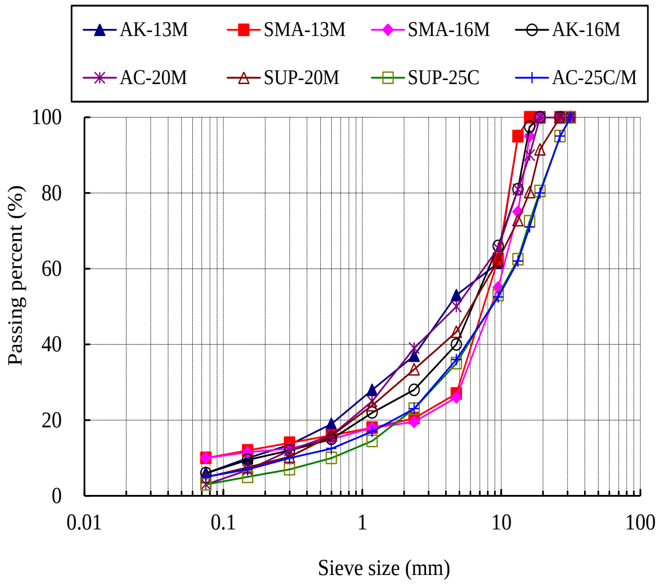

Fig. 3. Aggregate Gradations.

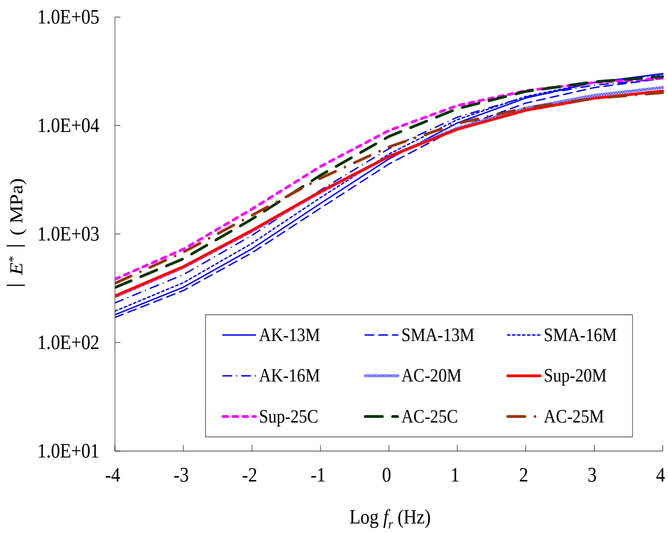

Fig. 4. Dynamic Modulus Master Curves.

Table 2. Regression Coefficients of Cohesion and Friction Angle Prediction Equations.

Mix Type	α_1	α_2	R^2	β_1	β_2	R^2
AK-13M	107115	-1.309	0.999	59.807	-0.098	0.921
SMA-13M	96962	-1.298	0.998	131.720	-0.271	0.953
SMA-16M	65807	-1.198	0.999	107.930	-0.209	0.935
AK-16M	133306	-1.371	0.993	43.375	-0.030	0.927
AC-20M	172199	-1.439	0.993	169.650	-0.372	0.958
Sup-20M	235498	-1.541	0.991	96.051	-0.205	0.959
Sup-25C	433815	-1.820	0.992	63.590	-0.079	0.972
AC-25C	385832	-1.773	0.999	84.057	-0.158	0.988
AC-25M	107593	-1.345	0.989	57.425	-0.060	0.999

Damage Accumulation Law

The prediction was based on an incremental damage approach with analysis interval of one month. The strain-hardening procedure [16]

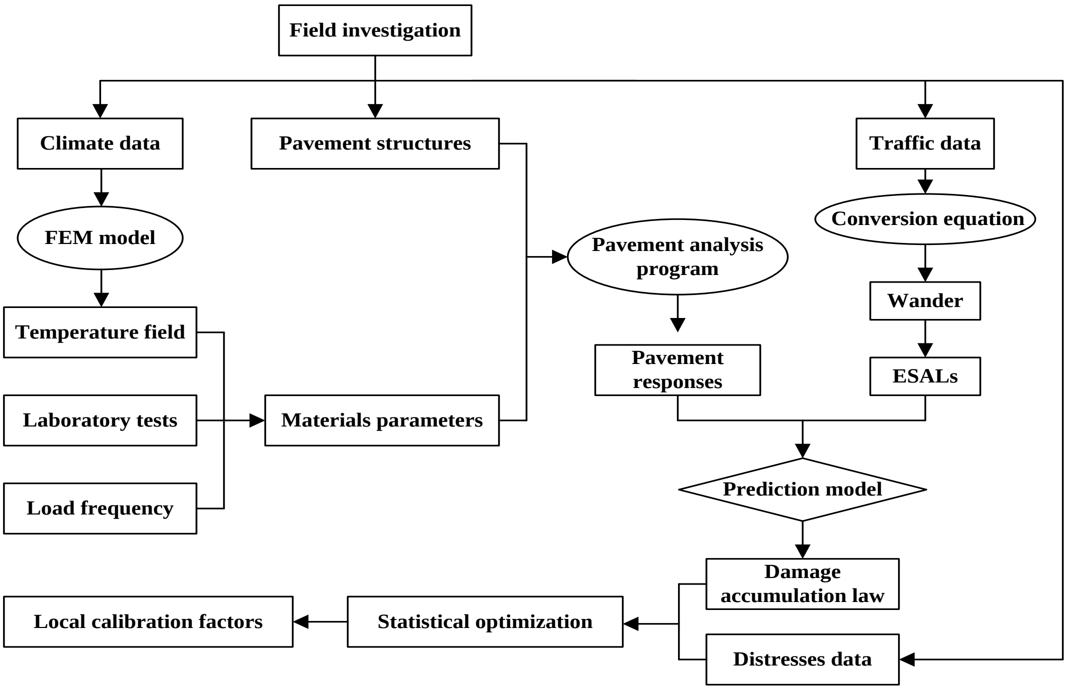

Fig. 5. Flowchart of the Calibration Procedure.

was employed to accumulate the permanent deformation in different periods.

Pavement Temperature Field

Temperature is an important input parameter in pavement design [17]. It can significantly affect the mechanical properties of asphalt mixtures, consequently affecting the pavement responses. Therefore, it is necessary to accurately characterize pavement temperature as a function of time and depth. In this study, the daily maximum and minimum temperatures were directly collected. However, only using the average temperature value will not capture the damage caused by the extreme temperatures. To solve this problem, a transient pavement temperature field FEM model based on heat transfer theory was employed to predict the hourly pavement temperature at each depth in each analysis period, as seen in Fig. 6. The required environmental parameters including air temperature, amount of solar radiation, effective sunshine duration, and average wind speed were obtained from field investigation. The thermodynamic parameters specific heat capacity C and thermal conductivity λ for different materials were measured in laboratory, as shown in Table 3. To account for the effect of extreme temperatures, the temperature frequency distribution was introduced [5]. The hourly pavement temperature field over an interval (one month) was calculated using the FEM model. The frequency distribution of temperature data was assumed to be normally distributed. The temperatures over one month are divided into five different sub-seasons. For each sub-season the temperature is

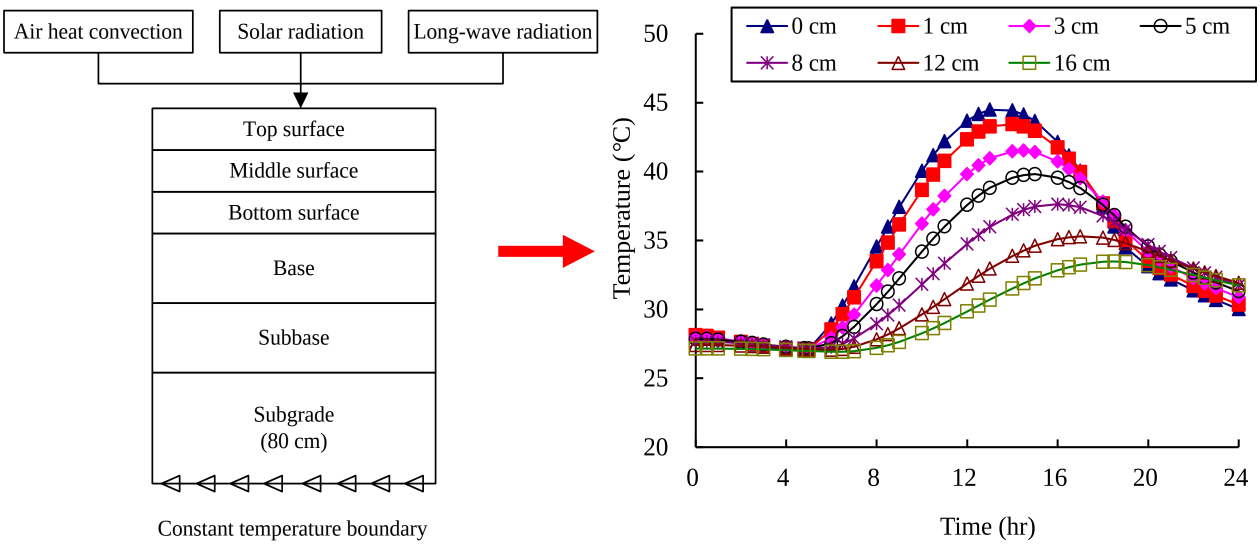

Fig. 6. Prediction of Pavement Temperature Field Using the FEM Model.

Table 3. Thermodynamic Parameters of Different Materials.

Parameter	Layer	10℃	20℃	30℃	40℃	50℃	60℃	70℃
C (J/kg·℃)	Top Surface	1124	1188	1271	1326	1356	1374	1374
	Middle Surface	924	942	961	985	1015	1036	1047
	Bottom Surface	928	947	970	997	1026	1046	1056
	Base/Subbase				810			
	Subgrade				860			
λ (J/m·h·℃)	Top Surface	5327	5635	6025	6285	6427	6515	6516
	Middle Surface	5664	5776	5889	6041	6220	6350	6419
	Bottom Surface	5651	5766	5904	6071	6244	6368	6429
	Base/Subbase				3960			
	Subgrade				4680			

defined by a temperature that represents 20% of the frequency distribution for pavement temperature. The temperatures corresponding to the 10, 30, 50, 70, and 90 percentiles of the frequency distribution were used to identify five sub-seasons over a given interval. In each sub-season, it was assumed that 20% of the monthly traffic occurred. The pavement responses under each sub-season should be individually calculated.

Conversion of Axle Load

The equivalent single axle load (ESAL) approach was used for traffic characterization in this study. The 100 kN single axle dual tires load was selected as the standard axle load according to the Chinese criterion [18].

From laboratory tests data [9], the relationship of load magnitude and the ratio of shear stress to strength was obtained.

$$\frac{(\tau/\tau_f)_1}{(\tau/\tau_f)_2} = (\frac{P_1}{P_2})^m \tag{5}$$

where P_1 is axle load 1, kN; P_2 is axle load 2, kN; $(\tau/\tau_f)_1$ is the ratio of shear stress to strength under axle load 1; $(\tau/\tau_f)_2$ is the ratio of shear stress to strength under axle load 2; m is the regression coefficient.

To produce the same magnitude of permanent deformation, the following equation could be obtained.

$$\tau/\tau_f = a\left(N_f\right)^{-b} \tag{6}$$

where N_f is the fatigue life corresponding to a given level of permanent deformation; a and b are the constant regression coefficients, which could be obtained for different mixtures at different test conditions. Combining Eq. (5) and Eq. (6), it was observed that:

$$(\frac{P_1}{P_2})^m = \frac{(\tau/\tau_f)_1}{(\tau/\tau_f)_2} = \frac{a(N_{f1})^{-b}}{a(N_{f2})^{-b}} = (\frac{N_{f1}}{N_{f2}})^{-b} \tag{7}$$

$$\frac{N_{f1}}{N_{f2}} = (\frac{P_2}{P_1})^{\frac{-m}{-b}} = (\frac{P_2}{P_1})^n \tag{8}$$

where N_{f1} is the fatigue life corresponding to a given level of permanent deformation under the axle load P_1; N_{f2} is the fatigue life corresponding to a given level of permanent deformation under the axle load P_2; n is the conversion coefficient of axle load.

The Eq. (8) is only valid for the load conversion between the same axle types. To consider the effects of different axle types, the following conversion equation of axle load based on rutting equivalent principle was finally developed.

$$\frac{N_{f1}}{N_{f2}} = C(\frac{P_2}{P_1})^n \tag{9}$$

where C is the axle type coefficient, representing the ratio of permanent deformation produced between other axle types (tandem and tridem axles) and standard single axle with the same load magnitude.

According to laboratory tests data and pavement responses, the coefficients of m, b, n, and C were obtained for different mixtures [19], as seen in Table 4. The conversion coefficient of axle load n of 4.00 was finally selected for calculation.

Traffic Wander

Traffic wander is the lateral distribution of axle loads. It plays a direct and significant role in affecting the permanent deformation in asphalt pavements [20]. The direction distribution, lane distribution, and wander factors was used in this study to correct the number of loads over a specific point investigated in pavement surface. The direction and lane distribution factors could be directly obtained from field investigation. To reflect the effects of lane width on wander, the wander factor was used. The final wander (20.3 cm) was the product of wander factor (0.8 corresponding to the lane width of 3.75 m) and default wander (25.4 cm) [5].

Load Frequency Distribution

The response of deformation in asphalt concrete shows delayed behavior from the applied loading time due to its time dependence [21]. The load frequency/duration is a main parameter to determine the dynamic modulus. It also has been incorporated into the proposed prediction model (Eq. (2)) as a required input parameter. The load frequencies at different pavement depths were calculated using the relationships developed from field tests [22]. The average

Table 4. Coefficients for Conversion Equation of Axle Load [19].

Coefficient	m	b	N	C		
				Single	Tandem	Tridem
Value	0.78-0.99	0.23	3.39-4.30	1.00	0.12	0.03

speed of 80 km/h for the trucks was used. The effects of rest periods were not specially considered due to the lack of field data.

Pavement Responses Calculation

The multilayered elastic program KENLAYER was used to calculate pavement responses, mainly principal stresses as shown in Eq. (1) in this study. The pavement structures of all sections are listed in Table 1. A simplified procedure with three analysis points was used to determine the critical locations with respect to permanent deformation [23]. Elastic modulus and Poisson's ratio are the two main material parameters used in KENLAYER. The dynamic modulus values of asphalt mixtures were determined from Fig. 4 in each sub-season. Constant elastic modulus values typically used in China of 4,000 MPa, 2,000 MPa, and 150 MPa were assumed for base, subbase, and subgrade for entire analysis period, respectively. Poisson's ratio values of 0.35, 0.20, 0.25, and 0.35 were used for asphalt concrete layers, base, subbase, and subgrade, respectively. Cohesion and friction angle for each asphalt concrete layers were calculated using Eqs. (3) and (4). The ratio of shear stress to strength was calculated using Eq. (1). It was assumed that asphalt concrete layers contributed 100% of total permanent deformation in the entire pavement since semi-rigid base and subbase were selected in all sections [24]. A sublayering summation method was used for a more accurate calculation. The asphalt concrete layer (including top, middle, and bottom surface layers as shown in Table 1) was divided into several sublayers. Each asphalt concrete sublayer has 20-30 mm thickness. The thickness of the sublayer in the upper portion of the asphalt concrete layer (20 mm) is smaller than that in the lower portion of the asphalt concrete layer (30 mm) since more permanent deformation occurs in the upper portion. The permanent deformation in each sublayer was predicted and then summed to determine the permanent deformation in the entire asphalt concrete layer [25].

Statistical Optimization

Based on the primary laboratorial model as shown in Eq. (2), the following final form of prediction model was established with the calibration factors to consider local conditions.

$$\varepsilon_p = k_1 \cdot 9.2675\times10^{-3} e^{k_2 \cdot 6.2807\times10^{-6} N} e^{k_3 \cdot 3.6723 \frac{\tau}{\tau_f} N^{k_4 \cdot 0.1032}} t^{k_5 \cdot 0.4224} \tag{10}$$

where k_1, k_2, k_3, k_4, and k_5 are local calibration factors.

The following three-step procedure was employed to make this calibration:

(1) Determination of k_5. k_5 captures the differences arising from load duration between laboratory test and field. It was fixed as 1.0 at this step since load duration data was unavailable from field investigation.

(2) Determination of k_2, k_3, and k_4. k_2 and k_4 modify the differences arising from load cycles while k_3 considers the effects of both load cycles and the ratio of shear stress to strength (a function of pavement structures and materials). Because multiple optimal solutions can exist due to more than one decision variable, 64 possible combinations (4×4×4) of k_2, k_3, and k_4 were designed after trial calculation to avoid from producing unreasonable calibration factors. The four levels assumed for each local calibration factor are listed in Table 5.

k_1 was fixed at a certain value of 1.0 at this step since it did not have effects on the optimum combination of k_2, k_3, and k_4. The permanent deformation was predicted with each combination of calibration factors for all sections. The optimum combination should minimize the sum of squared errors (SSE) between predicted and measured values. The 3D curves shown in Fig. 7 describe the variations of the SSE values along with the k_2 and k_3 at different levels of k_4. It can be found that the SSE value greatly varies with local calibration factors, from 17.66 to 128.18. The optimum combination to obtain the minimum SSE (17.66) is $k_2 = 0.002$, $k_3 = 0.01$, and $k_4 = 2.0$.

(3) Determination of k_1. k_1 is a shift factor to minimize the discrepancy between the predicted and the measured permanent deformation.

By using Microsoft Excel Solver function, the final local calibration factors $k_1 = 354.67$, $k_2 = 0.002$, $k_3 = 0.01$, $k_4 = 2.0$, and $k_5 = 1.0$ were selected. It is shown in Fig. 8 that the comparison of the measured and predicted rut depths using the proposed permanent deformation model after calibration for all analysis points. It is seen in the figure that the match is fairly good.

Validation

The remaining 4 pavement sections from the Yanjiang (YJ) highway were used to validate the final calibrated permanent deformation model. The validation results are presented in Fig. 9. The fluctuations of measured rut depths along with the time were mainly caused by two different methods of rutting measurement respectively used in the earlier and later periods. It is found from the figures that the locally calibrated model provide a reasonable prediction of permanent deformation for various asphalt pavements in Jiangsu of China. The average relative error of 12.5% can satisfy the accuracy requirement in engineering practice.

Table 5. Four Assumed Levels for Local Calibration Factors.

Local Calibration	Level			
Factor	1	2	3	4
k_2	0.001	0.002	0.003	0.004
k_3	0.005	0.010	0.015	0.020
k_4	1.0	1.5	2.0	2.5

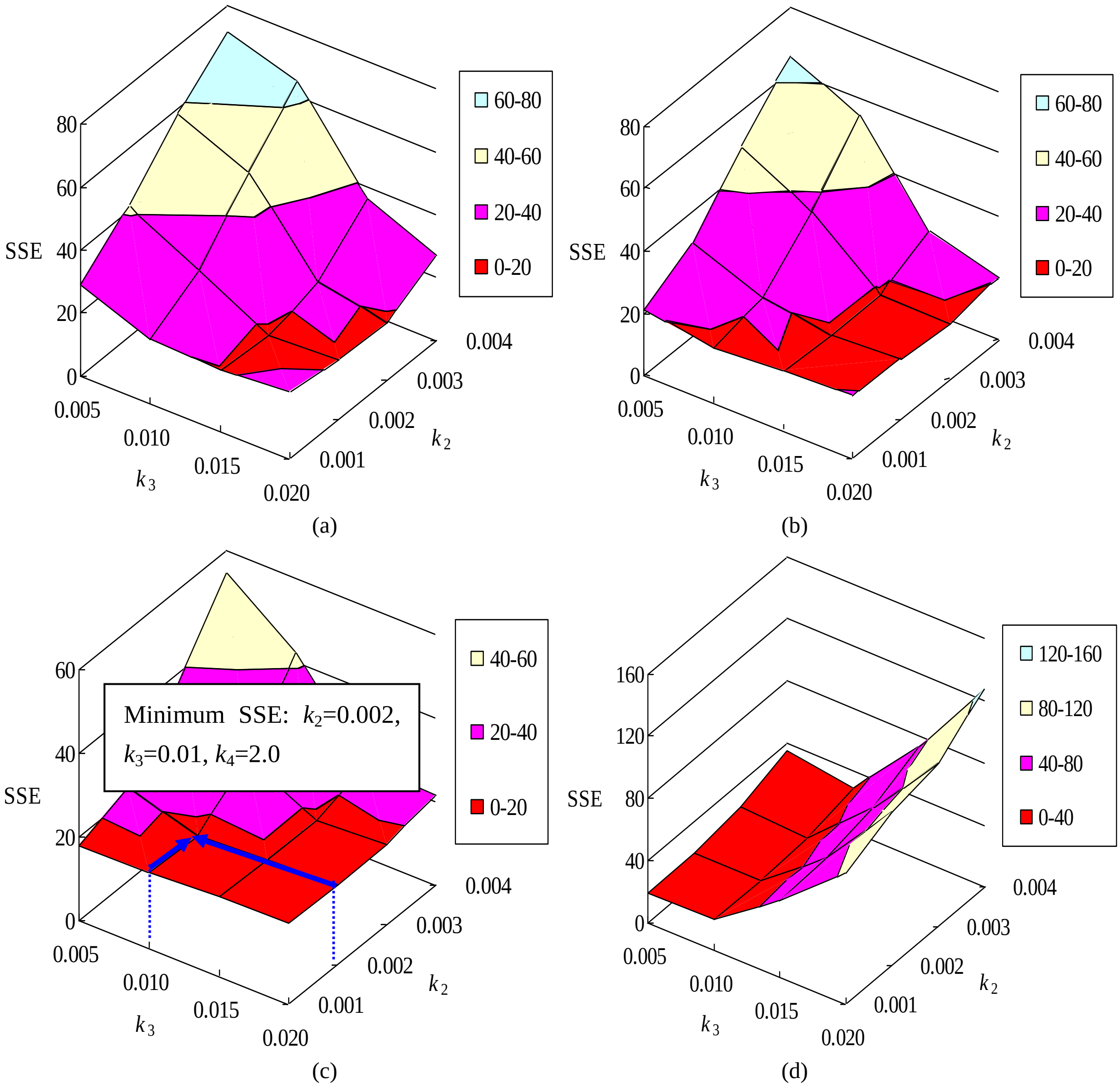

Fig. 7. SSE for Different Combinations of Calibration Factors: (a) k_4 = 1.0, (b) k_4 = 1.5; (c) k_4 = 2.0, and (d) k_4 = 2.5.

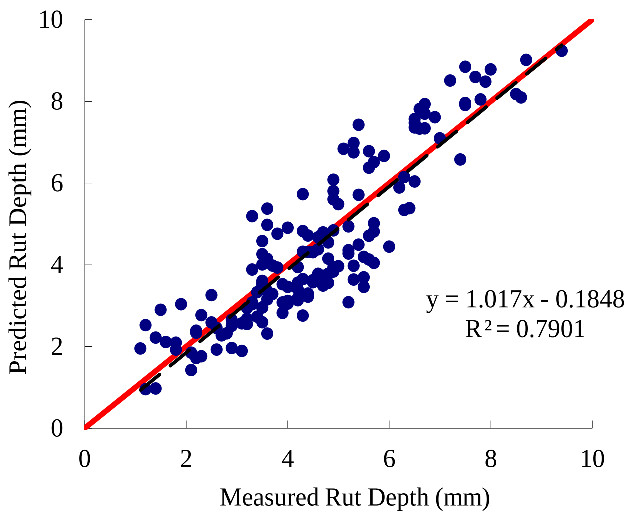

Fig. 8. Comparison of Measured and Predicted Rut Depths after Calibration.

Conclusions

This paper has summarized the research results of calibrating and validating a laboratory permanent deformation model of asphalt concrete based on shear properties using the long-term field data. The transient FEM pavement temperature field model, sub-season concept, traffic wander, and load frequency distribution was used in the three-step calibration procedure to link the laboratory and field conditions. A conversion equation of axle load to calculate ESALs was also proposed. The optimum combination of calibration factors for highways in Jiangsu of China was finally obtained by minimizing the SSE between the predicted and the measured permanent deformation.

It is found that the locally calibrated model can provide a reasonable prediction of permanent deformation for various asphalt pavements and satisfy the accuracy requirement in engineering practice. The reason may be that the dynamic modulus is the only material parameter for asphalt concrete in other models. By

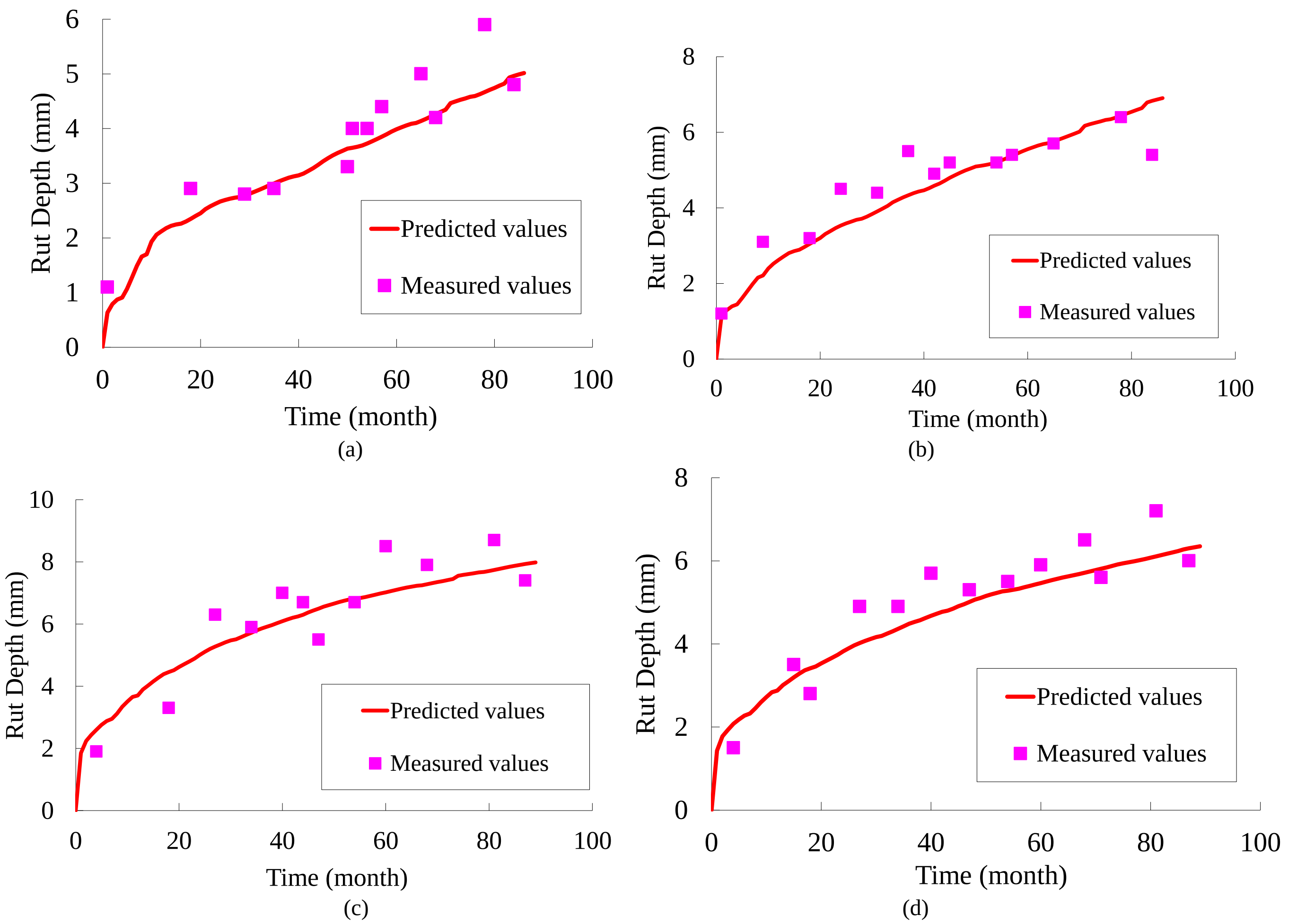

Fig. 9. Results of Validation Research for (a) Section YJ-1, (b) Section YJ-2, (c) Section YJ-3, and (d) Section YJ-4.

comparison, shear strength parameters (cohesion and friction angle), which are fundamental parameters representing the rutting resistance of asphalt concrete, are also required in the proposed model. Moreover, the ratio of shear stress to strength has the potential to take care of the effect of temperature, load frequency, and load magnitude.

It should be noted here that the sections investigated in this study have the same pavement grade and similar pavement structure. A further study is required to validate the model in a wide range of pavement structures and materials. Also, load duration data are unavailable from field investigation at this stage. Therefore, the local calibration factors k5 should be corrected in future.

Acknowledgements

This work is supported by Project supported by the National Natural Science Foundation of China (Grant No. 51308303), Natural Science Foundation of Jiangsu Province of China (Grant No. BK20130980), Specialized Research Fund for the Doctoral Program of Higher Education (Grant No. 20123204120011), Science and Technology Project by Ministry of Housing and Urban-Rural Development of China (Grant No. 2013-K4-9). Their financial support is much appreciated.

References

1. Hu, S., Zhou, F., and Scullion, T. (2011). Development, Calibration, and Validation of a New M-E Rutting Model for HMA Overlay Design and Analysis. *Journal of Materials in Civil Engineering*, 23(2), pp. 89–99.
2. Ziari, H. and Divandari, H. (2013). Presenting Asphalt Mixtures Flow Number Prediction Model Using Gyratory Curves. *International Journal of Civil Engineering*, 11(2), pp. 125–133.
3. Witczak, M.W., Kaloush, K., Pellinen, T., and El-Basyouny, M. (2002). Simple Performance Test for Superpave Mix Design. *NCHRP Report 465*, Transportation Research Board of the National Academies, Washington, DC, USA.
4. Zhou, F., Scullion, T., and Sun, L. (2004). Verification and Modeling of Three-Stage Permanent Deformation Behavior of Asphalt Mixes. *Journal of Transportation Engineering*, 130(4), pp. 486–494.
5. ARA, Inc., ERES Consultants Division. (2004). Guide for Mechanistic-Empirical Design of New and Rehabilitated Pavement Structures. Final report, NCHRP Project 1-37A, Transportation Research Board of the National Academies, Washington, DC, USA.
6. Freire, A.C., Antunes, M.L., and Luís de Picado-Santos.

(2006). Characterization of Bituminous Mixtures for Numerical Modeling of Permanent Deformations. *Road Materials and Pavement Design*, 7(1), pp. 87–102.
7. Said, S.F., Hakim, H., Oscarsson, E., and Hjort, M. (2011). Prediction of Flow Rutting in Asphalt Concrete Layers. *International Journal of Pavement Engineering*, 12(6), pp. 519–532.
8. Li, Q., Lee, H.J., and Hwang, E.Y. (2010). Characterization of Permanent Deformation of Asphalt Mixtures Based on Shear Properties. *Transportation Research Record*, 2181, pp. 1–10.
9. Li, Q., Lee, H.J., and Lee, S.Y. (2011). Permanent Deformation Model Based on Shear Properties of Asphalt Mixtures: Development and Calibration. *Transportation Research Record*, 2210, pp. 81–89.
10. Suh, Y.C., Cho, N.H., and Mun, S. (2011). Development of Mechanistic-empirical Design Method for an Asphalt Pavement Rutting Model Using APT. *Construction and Building Materials*, 25(4), pp. 1685–1690.
11. Kim S., Ceylan, H., Gopalakrishnan, K., and Smadi, O. (2010). Use of Pavement Management Information System for Verification of Mechanistic-Empirical Pavement Design Guide Performance Predictions. *Transportation Research Record*, 2153, pp. 30–39.
12. Hall, K.D., Xiao, D.X., and Wang, K.C.P. (2011). Calibration of the Mechanistic-empirical Pavement Design Guide for Flexible Pavement Design in Arkansas. *Transportation Research Record*, 2226, pp. 135–141.
13. Muthadi, N.R. and Kim, Y.R. (2008). Local Calibration of Mechanistic–Empirical Pavement Design Guide for Flexible Pavement Design. *Transportation Research Record*, 2087, pp. 131–141.
14. Li, J. (2010). Rutting Investigation and Causes Analysis in Jinghu Expressway Yihuaijiang Section, Master thesis, Southeast University, Nanjing, China (in Chinese).
15. Li, Q., Ni, F., Li, G., and Wang, H. (2013). Evaluation of the Dynamic Modulus for Asphalt Mixtures with Varying Volumetric Properties. *International Journal of Pavement Research and Technology*, 6(3), pp. 197–204.
16. Yun, T. and Kim, Y.R. (2011). A Viscoplastic Constitutive Model for Hot Mix Asphalt in Compression at High Confining Pressure. *Construction and Building Materials*, 25(5), pp. 2733–2740.
17. Wang, F., Machemehl, R.B., and Popova, E. (2012). Toward Monte Carlo Simulation-Based Mechanistic-Empirical Prediction of Asphalt Pavement Performance. *Journal of Transportation Engineering*, 136(7), pp. 678–688.
18. Ministry of Transport of the People’s Republic of China. (2007). Specifications for Design of Highway Asphalt Pavement, JTG D50-2006, Ministry of Transport, China (in Chinese).
19. Li, Q., Ni, F., and Li, G. (2013). Conversion Method of Axle Load for Asphalt Pavements Based on the Rutting Equivalent. *Journal of Transportation Engineering and Information*, 11(4) , pp. 63-70 (in Chinese).
20. Le, A.T., Lee, H.J., Park, H.M., and Lee, S.Y. (2009). Development of a Permanent Deformation Model of Asphalt Mixtures for South Korean Pavement Design Guide. *Transportation Research Record*, 2095, pp. 45–52.
21. Lee, S.J, Seo, Y.G., and Kim, Y.R. (2006). Experimental Validation of Laboratory Performance Models using the Third Scale Accelerated Pavement Testing. *KSCE Journal of Civil Engineering*, 10(1), pp. 9–14.
22. Hajj, E.Y., Ulloa, A., Siddharthan, R., and Sebaaly, P.E. (2010). Estimation of Stress Conditions for the Flow Number Simple Performance Test. *Transportation Research Record*, 2181, pp. 67–78.
23. Le, A.T., Lee, H.J., Park, H.M., and Kim, T.W. (2011). Development of Korean Pavement Design Guide for Asphalt Pavements Based on the Mechanistic-Empirical Design Principle. *The Baltic Journal of Road and Bridge Engineering*, 6(3), pp. 169–176.
24. Wang, H., Li, X., Zhang, Q. (2009). Rutting in Asphalt Pavement Under Heavy Load and High Temperature. *China Civil Engineering Journal*, 42(5), pp. 139-144 (in Chinese).
25. Suh, Y.C., Park, D.W., Jo, N.H., and Kwon, S.A. (2012). Prediction of Permanent Deformation in Full-Scale Accelerated Pavement Testing. *KSCE Journal of Civil Engineering*, 16(4), pp. 579–585.